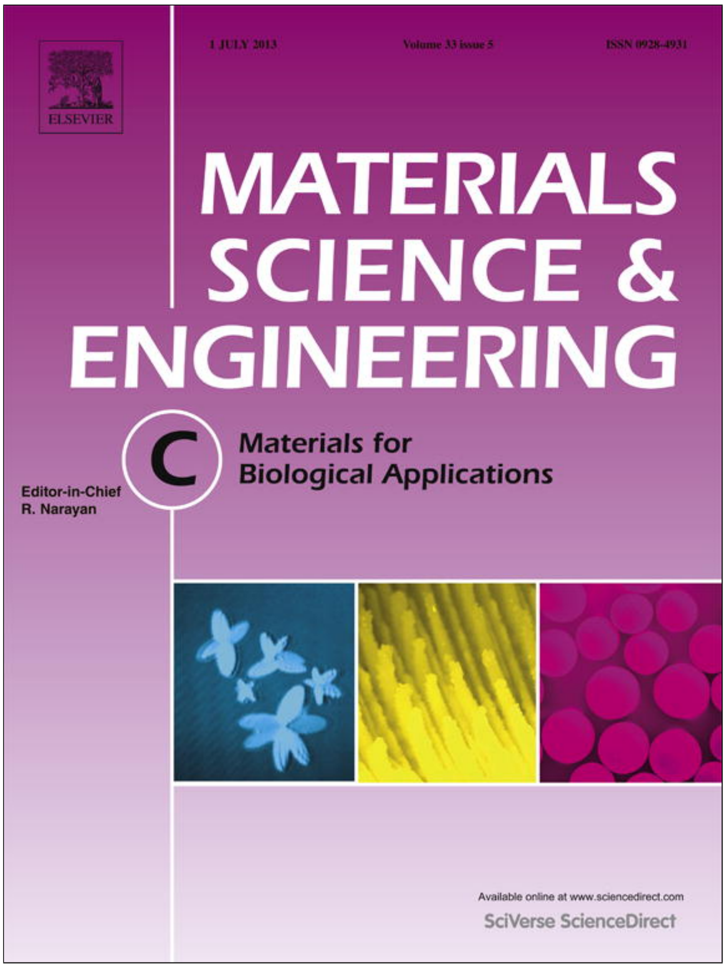
1 JULY 2013
Volume 33 issue 5
ISSN 0928-4931
ELSEVIER
MATERIALS SCIENCE & ENGINEERING
C
Materials for Biological Applications
Editor-in-Chief
R. Narayan
Available online at www.sciencedirect.com
SciVerse ScienceDirect

Materials Science and Engineering C 33 (2013) 2657–2663

Contents lists available at SciVerse ScienceDirect

Materials Science and Engineering C

journal homepage: www.elsevier.com/locate/msec

Analysis of percussion response of dental implants: An in vitro study

Andrew Dinh [a], Cherilyn G. Sheets [b], James C. Earthman [a,*]

[a] Department of Chemical Engineering and Materials Science, University of California, Irvine, CA 92697-2575, United States
[b] Newport Coast Oral–Facial Institute, 360 San Miguel, Suite 204, Newport Beach, CA 92660, United States

ARTICLE INFO

Article history:
Received 12 April 2012
Received in revised form 6 February 2013
Accepted 16 February 2013
Available online 22 February 2013

Keywords:
Dental implants
Percussion diagnostics
Computer tomography

ABSTRACT

The Periometer® quantitative percussion system was used to interrogate the interfacial stability of implants in vitro for comparison with X-ray computer tomography (CT) data. Selected implants were placed as per standard practice in bone stimulant polyurethane blocks. The dimensions of the surgical sites surrounding the implants were analyzed using X-ray computer tomography (CT) to determine the quality of support at the implant–bone interface. In particular, the misfit between the size of the surgical site and the corresponding implant was determined for each sample. The resulting average surgical site error from the CT scans was found to exhibit good agreement with the presence of irregularities found in the percussion data.

1. Introduction

Dental implants have been widely used for over 30 years and numerous companies provide multiple implant designs to treat edentulous or partially edentulous patients. The failure rates of these implants are relatively low, but depend greatly on the density and quality of bone at the implantation site [1–4]. It is believed that a greater initial stability of an implant indicates a higher probability of successful osseointegration [3,5]. One of two protocols for implantation is typically used to achieve osseointegration. The first protocol is the conventional two step process that calls for the surgical placement and suturing of the soft tissue over the implant to allow for healing, usually three to six months, before uncovering the implant and attaching the abutment [6,7]. This method generally provides for more predictable osseointegration by allowing the implant to integrate with the surrounding tissue before it is exposed to the forces associated with mastication and occlusion [7,8]. The second protocol involves either immediate (within 24 h) or early (after 24 h but before three months) loading of the implant after it has been surgically placed. Immediate and early loading of implants allows for mechanical forces resulting from mastication and occlusion to be transmitted to the bone in the hope of stimulating faster osseointegration of the implant at the cellular level [7,8]. The conventional protocol leads to reasonably high success rates of 96–100%. By contrast, immediate loading for a broad patient population can yield a 79–85% success rate [5,7–12]. Despite this shortcoming, immediate loading can lead to faster osseointegration as a result of the additional mechanical stimulus as long as it is not excessive. Thus, immediate loading could become the protocol of choice if methods are developed to decrease the risk of failure. We hypothesize that significant risk mitigation could be realized using quantitative percussion diagnostics to periodically assess the primary stability of the implant and the mechanical integrity of the underlying bone.

The Periotest unit was designed to measure periodontal stability of natural teeth using percussion loading. The instrument measures percussion time on an arbitrary scale that is expressed in PTVs (Periotest Values). The Periotest has provided some information for evaluation of the osseointegration process in the literature [13] but has not received widespread acceptance for several reasons. The most damaging criticism is that the Periotest gives inconsistent results. This inconsistency has been related to two factors: the measurement is affected by the position and direction of the probe that must be held 2 mm from the surface of the implant restoration and the resolution of the PTV scale is limited in range for implants resulting in a lack of sensitivity [14–19].

The Osstell Mentor uses a resonance frequency analysis (RFA) as an indicator of implant stability. The Osstell system does provide a more quantitative and reliable measurement of implant stability compared to the Periotest. However, the Osstell also has limitations: a specialized measuring device, "smart peg", must be attached directly to the implant at the fixture level, each implant design requires a different smart peg geometry for testing, the superstructure of the implant must be disassembled for each testing session and this disassembly can compromise the mucosal barrier resulting in the loss of connective tissue and bone [18–21]. Accordingly, this system has not realized widespread acceptance in the US.

Quantitative percussion diagnostics in dentistry has been further developed using the Periometer® (Perimetrics, LLC, Newport Beach, California 92660) [13]. This instrument consists of a

* Corresponding author. Tel.: +1 949 824 5018.
E-mail address: earthman@uci.edu (J.C. Earthman).

0928-4931/$ – see front matter © 2013 Elsevier B.V. All rights reserved.
http://dx.doi.org/10.1016/j.msec.2013.02.033

handheld probe that has an orientation indicator and a patented tip that is placed directly against the implant abutment or restoration. This innovation assures a reproducible spacing from and orientation with the surface of the test sample. In addition, this tip has a tab on one side that provides for consistent vertical positioning of the probe. Since the Periometer can be used on a healing abutment, impression abutment or a restoration on an implant without disassembly, it can be used at any stage of implant life from placement to final restoration lifetime monitoring. This capability offers a distinct advantage over RFA and other techniques that require disassembly while at the same time has been found to provide indications of implant stability that are comparable to RFA measured by the Osstell Mentor [22].

The handpiece taps a sample with 2 to 20 N maximum force depending on the mechanical properties of the test specimen. The Periometer handpiece delivers a free-floating tapping probe to the test site with a consistent kinetic energy of approximately 0.32 mJ just prior to each percussion of the sample. From the resulting data, the energy returned to the probe normalized by the kinetic energy of the probe prior to impact versus time is determined and analyzed [23]. This normalized energy return is then used to approximate a damping capacity parameter, the loss coefficient, for the structure.

The Periometer was used to characterize the overall stability of dental implants using the loss coefficient in a previous in vitro study performed by VanSchoiack et al. [23]. The loss coefficient is a damping capacity parameter that indicates the overall energy dissipation in a structure. The loss coefficient was found to increase as simulated bone block density decreased, as shown in Fig. 1. However, it was noted that loss coefficient values sometimes significantly varied from the observed trend and between seemingly identical pairs of specimens. This variability appeared to be associated with irregularities in the corresponding percussion response versus time data [23]. In the present work, the percussion response for samples that exhibited these irregularities was quantitatively analyzed and compared to data from computer tomography (CT) scans. The primary objective was to determine whether irregular features in the response data obtained with the Periometer correlate with the quality of the surgical site in simulated bone indicated by CT data.

2. Materials and methods

2.1. Sample configurations

Sawbones® (Pacific Research Laboratories, Inc., Vashon, WA) polyurethane foam blocks were used to model cancellous bone often found at implantation sites. Two distinct types of blocks with various densities were investigated; the first type had disconnected porosity, the closed-cell model, and the other type had interconnected porosity, the open-cell model. Each block had dimensions of $2.5 \times 2.5 \times 4$ cm. Four different titanium implant designs were used in the present study: Friadent Frialit-2 Synchro, Friadent XiVE, Nobel Biocare Branemark System MK IV, or Nobel Biocare Replace Select [23]. A dental implant was placed as specified by standard placement protocol in the center of the square face of each Sawbones® block. An identical pair of samples was created for each implant design and block density. Once the implants were placed, abutments were fastened to each implant using a 20 N cm torque driver. The Frialit-2 Gingiva Former abutment was used on the XiVE and Frialit implants, the Healing Abutment Bmk Syst RP was used on the Branemark implants, and the Healing Abutment Select RP was used on the Replace Select implants.

Two pairs of identical samples were included in the present study which exhibited percussion responses that were relatively similar in shape. This self-consistent group of samples consisted of two Friadent XiVE implants, each in a 641 kg/m^3 closed-cell Sawbones® simulated bone block and two Friadent Frialit-2 Synchro implants, each in a 240 kg/m^3 closed-cell Sawbones® block. Four more pairs of samples were included in the present work that exhibited energy return responses with dissimilar shapes within each pair despite the fact that the components within each pair were initially identical. These test samples included two Nobel Biocare Replace Select implants in the 641 kg/m^3 closed-cell blocks, two Friadent Frialit-2 Synchro implants in 320 kg/m^3 closed-cell blocks, two Nobel Biocare Branemark System implants in the 240 kg/m^3 closed-cell blocks, and two Friadent XiVE implants in 200 kg/m^3 open-cell blocks. The energy return responses for the XIVE implants in 641 kg/m^3 blocks were not only self-similar but also highly uniform in shape and, for this characteristic, serve as a control group for the other samples.

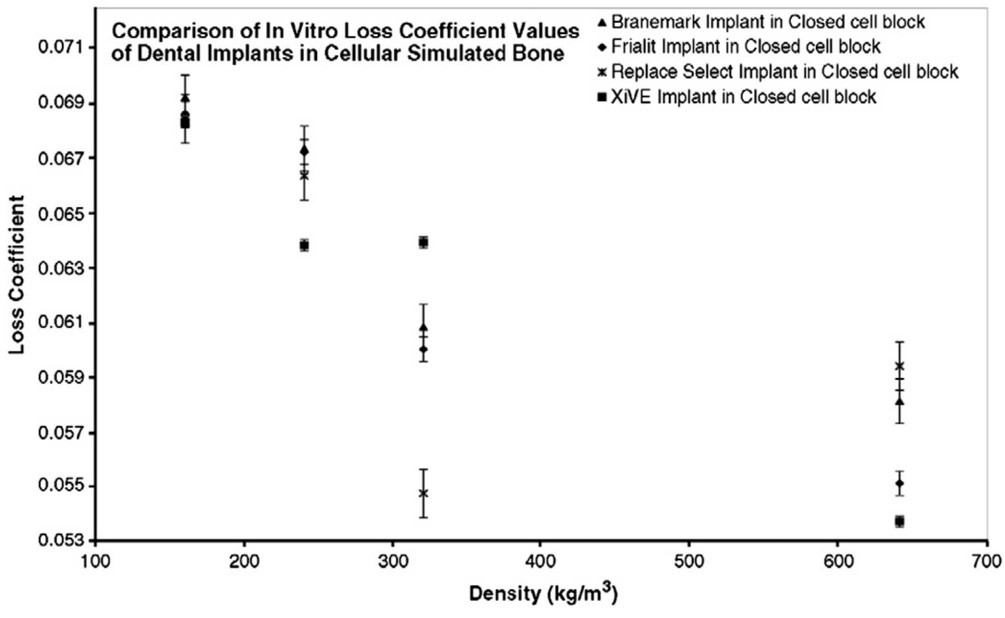

Fig. 1. Loss coefficient as a function of simulated bone block density for in vitro samples tested under percussion conditions reported by VanSchoiack et al. [23].

2.2. Percussion testing

Each sample was tested with the percussion probe against the abutment perpendicular to the implant axis in the same manner used by VanSchoiack and coworkers [23]. Ten sets of percussion response data were saved for each sample to assure reproducibility of the results. Further details on the percussion testing are given in [23].

2.3. Normal fit error (NFE)

Percussion response data for each of the samples under investigation were analyzed to determine a parameter that characterizes the shape of the percussion response versus time. A stress wave propagates through the Periometer probe upon its percussion with a specimen. Conservation of energy dictates that the mechanical energy experienced by the probe associated with this stress wave is given by

$$E_r = U - D \quad (1)$$

where U is the input energy equal to the kinetic energy of the probe just before impact, and D is the energy dissipated by the specimen. For Periometer testing, U is a constant in that the probe administers the same kinetic energy just prior to each percussion. The energy returned to the probe, E_r, as a function of time gives a quantitative description of the percussion response of the sample. The normalized energy return (NER) defined as E_r/U was then determined as a function of time to indicate the relative amount of energy conserved by the specimen. In analyzing the data for each sample, NER as a function of time characteristic of a defect-free sample was compared with the measured NER versus time using a nonlinear fit algorithm on a desktop computer. A normal fit error (NFE) can then be obtained by dividing the error between the defect-free response and the measured NER data by the overall amplitude of the data. The NFE indicates how much a given response deviates from that for a defect-free sample. Further details on how NFE values are determined are given in Appendix A.

NFE values were determined from 10 NER vs. time data sets for each sample in the present study and mean NFE values for each sample were also calculated. Analysis of variance (ANOVA) was performed to examine whether or not the mean value of the NFE was significantly different (P value < 0.05) for each identical pair of samples. Percussion tests were also performed on a fully solid polytetrafluoroethylene (PTFE) specimen that contains no porosity or irregularities to provide control data for the present study. A mean value of 0.0081 was measured for this defect-free sample, which serves as a baseline for the present in vitro implant specimens.

2.4. X-Ray computer tomography

X-Ray computer tomography was used in the present work to evaluate the integrity of the interface between each implant and corresponding foam block. In order to perform this determination, two issues had to be addressed. First, the polyurethane in the present foam blocks is essentially radio-transparent and therefore cannot be resolved using X-ray techniques. Second, X-rays are generally highly scattered by titanium implants. To overcome these issues, the implants in the present samples were carefully removed after percussion testing by reverse torque. The resulting unoccupied surgical site was then tightly packed with barium sulfate powder. Barium sulfate was chosen because it is radiopaque and, in powder form, can accurately fill void defects along the sides of the surgical site.

X-Ray computer tomography (CT) scans of the blocks containing barium sulfate were performed by using an i-CAT Precise CT system (Imaging Sciences International, LLC, Hatfield, PA). ImageJ software (National Institutes of Health, Bethesda, MD) was used to analyze the CT scan results to determine the cross sectional area of each implant surgical site along its entire length. Distance on the images was calibrated using the known block size for each model by placing a thin layer of $BaSO_4$ on the outside of the block. The calibration constant was determined to be 2.83 pixels/mm corresponding to a spatial resolution of 353 μm and a circular area resolution of 0.391 mm^2. A single 2D CT scan provided a horizontal cross-sectional view of the surgical site, as shown in Fig. 2. The surgical site area was determined by manually selecting the white portion at the center of the blocks, corresponding to where the $BaSO_4$ was located in the surgical site. This area was measured using ImageJ for at least 14 locations along the length of the surgical site. The cross sectional area profile of each implant was also determined by measuring its diameter at these locations using an electronic caliper. An interface error was then determined by subtracting the implant cross sectional area from the surgical site area over the length of the surgical site. A mean interface error was then recorded for each sample by averaging these surgical site errors.

3. Results and discussion

Percussion testing results in terms of the mean normal fit error for each identical sample pair are listed in Table 1. The standard deviation for each mean value is also listed in this table. We note that the standard deviations were always less than 8% of the corresponding mean NFE value with the exception of one specimen (Frialit/240 sample S1) in which the standard deviation was about 16% of the mean NFE value. The P value also listed in Table 1 indicates the probability that the mean values of the NFE are the same between the corresponding identical pair of samples. We note that the criterion for significant difference (P<0.05) is satisfied for the Branemark/240, XiVE/200 and Replace/641 samples despite the fact that they are identical pairs of samples. In the following, evidence from CT scans in conjunction with the percussion data is discussed that sheds some light on the cause of these differences.

3.1. Sample pairs with consistent NFE values

Representative normalized energy return (NER) data for the Friadent XiVE implants in 641 kg/m^3 closed-cell polyurethane blocks are shown as a function of time in Fig. 3a. We note that both sets of data exhibit peaks that are nearly symmetric and uniform in shape. Accordingly, the NFE values for these implants are relatively low, slightly below the baseline value for the PTFE control, and nearly

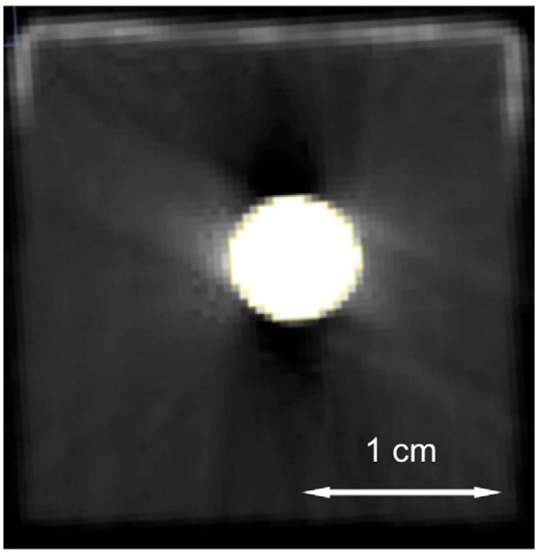

Fig. 2. A cross-sectional image obtained from a CT scan used in the present work. Only the purely white pixels at the implant site were considered part of the surgical site area.

Table 1
Mean normal fit error (NFE) with their corresponding standard deviations for identical pairs of in vitro implant samples.

Implants	Block density (kg/mm^3)	Normal fit error mean value	Standard deviation	*P* value
XiVE	641	0.0066	8.2×10^{-4}	0.187
		0.0071	7.9×10^{-4}	
Frialit-2	320	0.0130	8.4×10^{-4}	0.141
		0.0124	8.9×10^{-4}	
Frialit-2	240	0.0155	2.6×10^{-4}	0.099
		0.0171	9.5×10^{-4}	
Branemark Mk IV	240	0.0134	8.7×10^{-4}	1.82×10^{-6}
		0.0162	9.5×10^{-4}	
XiVE	200 (open-cell)	0.0135	6.9×10^{-4}	2.12×10^{-14}
		0.0216	9.4×10^{-4}	
Replace Select	641	0.0231	12.2×10^{-4}	2.84×10^{-18}
		0.0087	3.2×10^{-4}	

the same. As also shown in Fig. 3b, the areas of the surgical sites for this implant pair determined from CT scans were nearly identical to those for the implant indicating a tight fit with good support and no void defects along the interface. Close examination of the CT data showed that the implant model with the larger amplitude was also placed about 0.5 mm lower in the simulated bone block. This finding is reasonable since the slightly deeper placement of the implant would provide more support allowing for more energy return measured by the percussion probe.

Friadent Frialit implants in 320 kg/m^3 closed-cell blocks exhibited a large discrepancy in their NER amplitudes but a relatively small difference in NFE as shown in Fig. 4a. We note that the implant with the larger energy return amplitude corresponded to the larger NFE than the other implant in this pair. Analysis of the CT scans of the samples revealed that the implants were placed at nearly identical depths, but the implant with the larger amplitude had tighter support from the block over a large section near the apex of the implant (Fig. 4b). While this somewhat relaxed support over the apical region of the implant does not give rise to a greater NFE, it does reduce the overall amplitude of the NER. This difference in overall amplitude is reflected by the loss coefficient, a damping parameter that was examined earlier [23]. The small overall difference between the implant area and the measured surgical site areas for both samples in Fig. 4b was expected since the $BaSO_4$ was able to penetrate the pores in this lower density foam along the sides of the surgical sites, therefore making the surgical site area appear slightly larger in the CT scans.

Friadent Frialit implants in 240 kg/m^3 closed-cell blocks also exhibited somewhat similar energy return responses ($P=0.099$) and, as such, their NFE values were also similar as shown in Fig. 5a. However, both NFE values for the Frialit implants in 240 kg/m^3 blocks were greater than those for the XiVE and Frialit implants in higher density blocks shown in Table 1. This higher overall NFE can be attributed to the fact that a lower density block will have a greater chance of containing relatively large pores at the interface with the implant that could alter the response significantly. We note that the difference in the percussion responses in Fig. 5a can be justified by the slightly

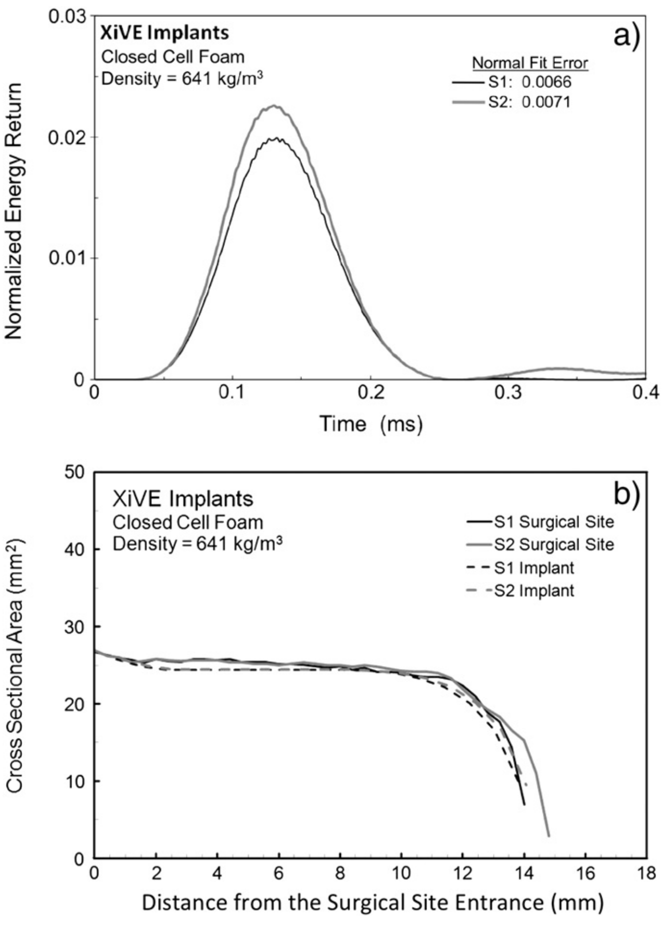

Fig. 3. (a) Normalized energy return versus time for a XiVE implant pair in a 641 kg/m^3 closed-cell simulated bone, and (b) areas of the surgical site for these samples, together with the measured implant cross sectional area (dashed lines), plotted against the distance from the entrance of the surgical site, where the crestal end of the implant was placed.

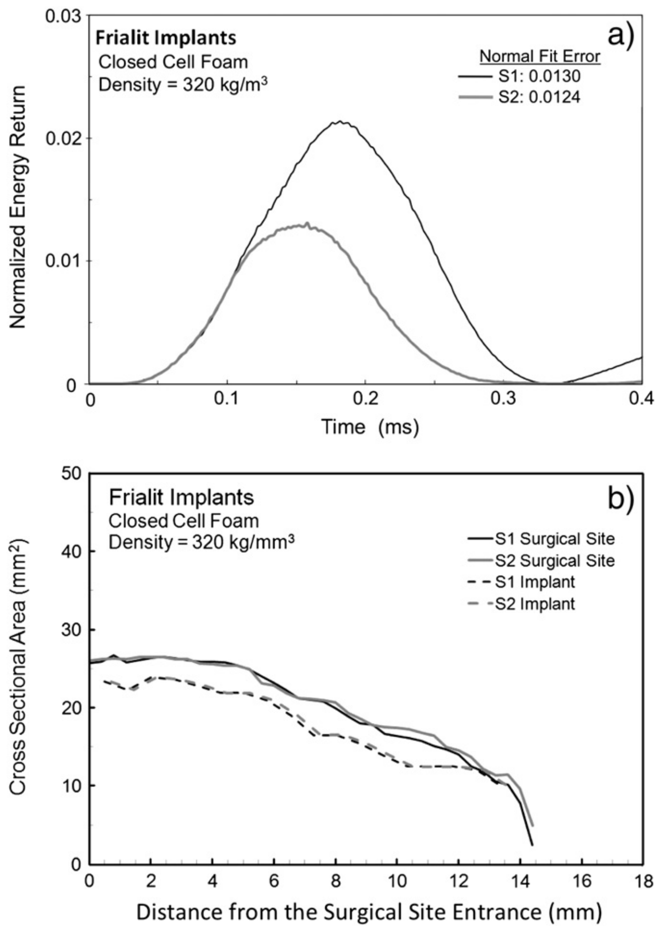

Fig. 4. (a) Normalized energy return versus time, and (b) area of the surgical site corresponding with the plotted implant dimensions (dashed lines) for two Frialit implants in 320 kg/m^3 closed-cell simulated bone.

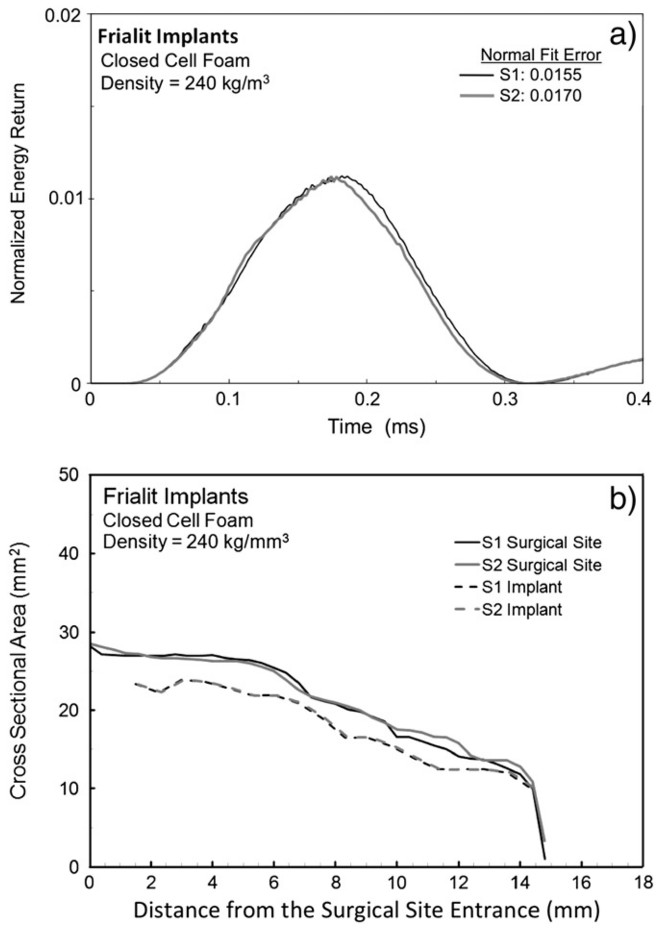

Fig. 5. (a) Normalized energy return versus time for a Frialit implant pair in a 240 kg/m^3 closed-cell simulated bone, and (b) areas of the surgical site for these samples plotted against distance from the entrance of the surgical site plotted together with the measured implant cross sectional area (dashed lines).

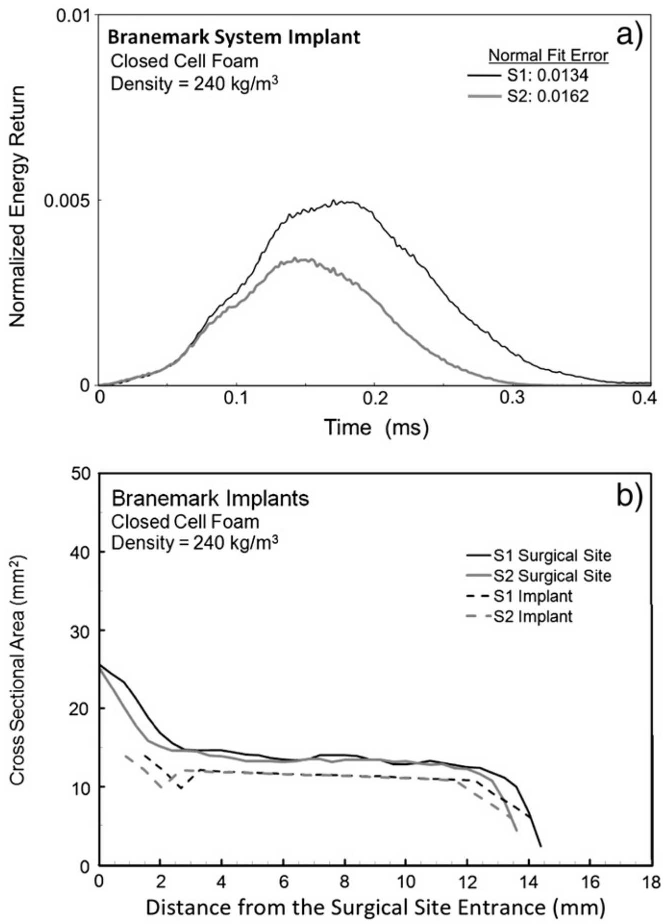

Fig. 6. (a) Normalized energy return versus time, and (b) area of the surgical site corresponding with the plotted implant dimensions (dashed lines) for two Branemark implants in a 240 kg/m^3 closed-cell simulated bone.

greater error between the surgical site area and the implant area near the apex of the implant for sample S2 in Fig. 5b.

3.2. Sample pairs with differing percussion responses

Normal fit error plotted against time for Nobel Biocare Branemark System implants in the 240 kg/m^3 closed-cell blocks is shown in Fig. 6a. One of these implants exhibited a normalized energy return response with significantly more abnormalities resulting in a larger NFE value compared to the replicate sample. The implant model with the larger normal fit error was placed lower and had a larger amplitude, but consistently had less support at the implant–bone interface, which is represented by a larger surgical site compared to that for the other implant as shown in Fig. 6b.

The results for XiVE samples in 200 kg/m^3 open-cell blocks are plotted in Fig. 7. It can be seen in this figure that one of these implants exhibited a relatively regular normalized energy return response while the other implant in the same density block exhibited more local instability as indicated by the perturbations in the response (Fig. 7a). Consequently, the implant with the more irregular NER response, sample S2, gave rise to a larger normal fit error. This sample also consistently exhibited a larger surgical site area along the length of the implant (Fig. 7b). This greater area could be a result of operator error when placing the implant or the random presence of a large pore at the implant in this relatively low density open-cell block. Inspection of Fig. 7b suggests that the larger NFE was a result of large pores due to the non-uniform fluctuation in surgical site area. In addition, the implant with the more uniform energy return response was placed about a millimeter lower than the other implant, which could provide the implant with more overall stability.

A Replace Select implant (S2) placed in a 641 kg/m^3 block exhibited a relatively low NFE value while that for its replicate sample (S1) was substantially greater as shown in Fig. 8a. Analysis of the CT scans of the two models revealed that, despite being placed further into the block, the implant with the higher NFE consistently exhibited a larger difference between surgical site area and implant area compared to that for the other implant in this pair, particularly near the crest and apex of the implant (Fig. 8b). The gradual increase in this difference toward both the crest and the apex suggests that the discrepancy in NFE values for this sample pair was due to operator error in the surgical placement for one of the implants.

A comprehensive comparison of the present results is shown in Fig. 9 as the normal fit error versus the mean surgical site error, the average difference between the measured surgical site area and the implant cross sectional area over the length of the implant. It can be seen in this figure that there is a general trend of lower normal fit error with a lower average surgical site error. The open-cell blocks correspond to the largest mean surgical site error since those blocks contained large interconnected pores that ranged from 0.5 to 1.5 mm in diameter according to manufacturer specifications.

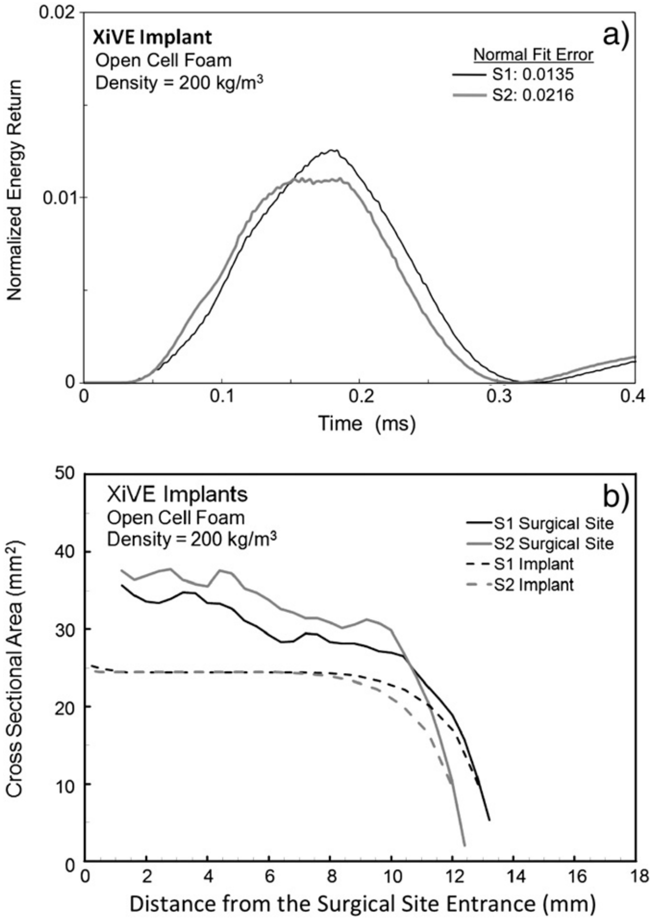

Fig. 7. (a) Normalized energy return curve for a XiVE implant pair of samples in a 200 kg/m^3 open-cell simulated bone blocks, and (b) area of the surgical site plotted together with the implant dimensions (dashed lines) as a function of distance from the entrance of the surgical site.

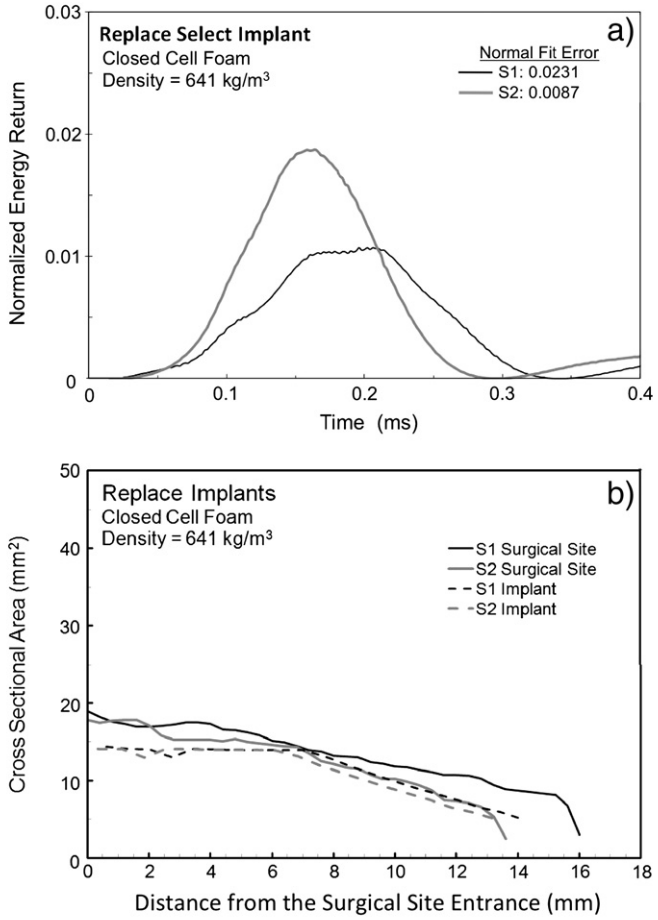

Fig. 8. (a) Normalized energy return curve for a Replace Select implant pair in a 641 kg/m^3 simulated bone model, and (b) area of the surgical site plotted together with the implant dimensions (dashed lines) as a function of distance from the surgical site entrance.

4. Conclusions

Percussion diagnostics has been used to assess the integrity of the support of implants placed in a bone stimulant material. Irregularities in the energy return responses, resulting in a larger normal fit error (NFE), can be attributed to defects along the bone–implant interface and a poorer support of the implant by the bone model. This correlation was observed in the analysis of the CT scans, where a lower NFE was also linked to a lower mean difference between the surgical site area and the corresponding cross sectional area of the implant. These findings indicate that the Periometer is capable of detecting defects along an implant at the bone–implant interface. Further studies are needed to determine the critical NFE value in which an implant should be deemed acceptable for loading.

Acknowledgment

The authors wish to thank Craig Scholz of Orbit Oral–Maxillofacial Imaging & Diagnostic Services, Newport Beach, CA for the use of the i-CAT Precise CT system used in the present work. Assistance with data analysis by Vaibhav Bajaj and Philip Choi is also thankfully acknowledged. The authors are also grateful to Dentsply and Nobel Biocare for their support in providing the implants for the present work and with implant placement in the simulated bone models.

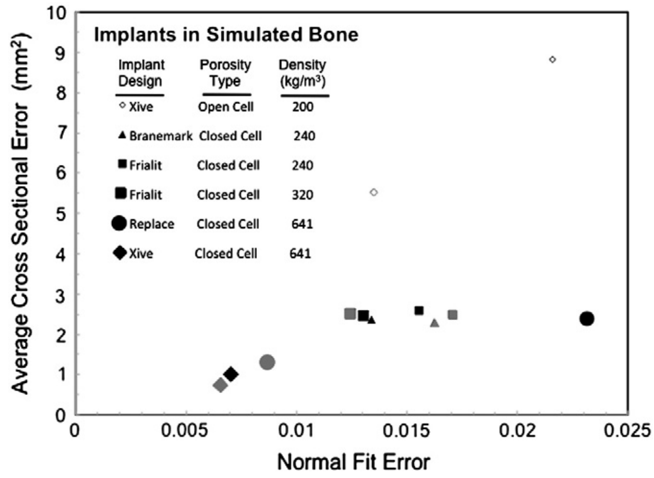

Fig. 9. Average cross sectional error, the mean difference between the surgical site area and the corresponding implant cross sectional area, plotted against normal fit error obtained from percussion data. Larger symbols represent denser simulated bone models and the closed symbols correspond to closed-cell simulated bone while the open symbols correspond to open-cell simulated bone.

Appendix A

Force variation resulting from Periometer percussion is determined by a sensor in the handpiece [23]. The energy return, E_r, characterizes the

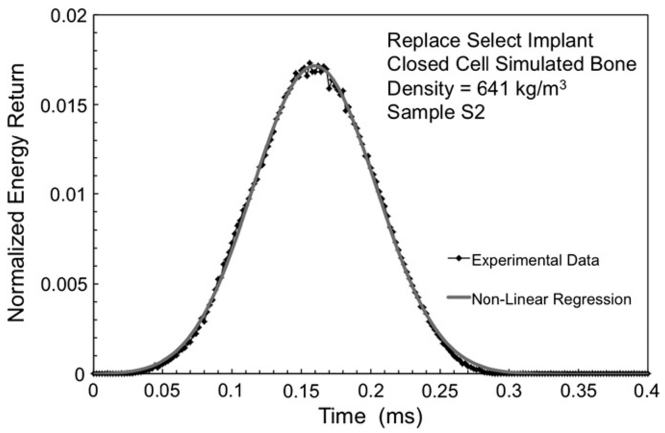

Fig. A1. Normalized energy return as a function of time for the Replace/641 sample S2 plotted together with the corresponding non-linear fit of Eq. (A2) to the data.

elastic energy of this force according to

$$E_r = \frac{F^2}{2k} \tag{A1}$$

where F is the resultant percussion force and k is the stiffness of the percussion rod assembly. The normalized energy return, $\overline{E}_r$, is the mechanical energy experienced by the percussion rod during impact divided by its kinetic energy just prior to contact with the sample. The resulting energy return peak for a defect-free sample has the approximate shape of a peak given by the following:

$$\overline{E}_r = \beta \sin^2(\gamma t) \exp\left[-\frac{(t-\phi)^2}{\psi}\right] \tag{A2}$$

where t is time, and β, γ, ϕ, and ψ are parameters that are determined via a nonlinear regression fit to experimental data using the Levenberg–Marquardt algorithm [24].

A nonlinear regression fit of Eq. (A2) to 10 energy return data sets was performed for each implant–block specimen in the present study. An example of a resulting fit plotted together with the corresponding NER data is shown in Fig. A1. A normal fit error, NFE, was obtained by dividing the resulting mean residue, average error of the fitted model to all ten data sets, by the amplitude of the fit to the data. This normalization of the mean error with the peak amplitude is justified by the observation that defects have a greater effect on distorting energy return peaks that have higher amplitudes. It is also reasonable that a greater distortion in the mechanical response results when more energy is available to drive the localized movements associated with a localized defect.

References

[1] P.K. Moy, D. Medina, V. Shetty, M. Dent, T.L. Aghaloo, Int. J. Oral Maxillofac. Implants 20 (2005) 569–577.
[2] M. Bischof, R. Nedir, S. Szmukler-Moncler, J.P. Bernard, J. Samson, Clin. Oral Implants Res. 15 (2004) 520–528.
[3] H. Martinez, M. Davarpanah, P. Missika, R. Celletti, R. Lazzara, Clin. Oral Implants Res. 12 (2001) 423–432.
[4] H.L. Huang, Y.Y. Chang, D.J. Lin, Y.F. Li, K.T. Chen, J.T. Hsu, Clin. Oral Implants Res. 20 (2011) 691–698.
[5] F. Javed, G.E. Romanos, J. Dent. 38 (2010) 612–620.
[6] I. Ericsson, K. Randow, K. Nilner, A. Peterson, Clin. Implant Dent. Relat. Res. 2 (2000) 70–77.
[7] A. Zembic, R. Glauser, A. Khraisat, C.H.F. Hammerle, Clin. Oral Implants Res. 21 (2010) 481–489.
[8] M. Degidi, A. Piattelli, J. Oral Implantol. 31 (2005) 25–31.
[9] R. Gapski, H.L. Wang, P. Mascarenhas, N.P. Lang, Clin. Oral Implants Res. 14 (2003) 515–527.
[10] B.A. Jung, W. Harzer, W. Gedrange, M. Kunkel, M. Moergel, P. Diedrich, G. Ludicke, H. Wehrbein, J. Orofac. Orthop. 71 (2010) 273.S–280.S.
[11] A. Rocci, M. Martignoni, J. Gottlow, Clin. Implant Dent. Relat. Res. 5 (2003) 29–36.
[12] I. Turkyilmaz, T.F. Tozum, C. Tumer, Clin. Implant Dent. Relat. Res. 12 (2010) 39–46.
[13] S. Winkler, H.F. Morris, J.R. Spray, J. Oral Implantol. 27 (2001) 198–203.
[14] N. Meredith, Crit. Rev. Biomed. Eng. 26 (1998) 275–291.
[15] N. Meredith, B. Friberg, L. Sennerby, C. Aparicio, Int. J. Prosthodont. 11 (1998) 269–275.
[16] L.C. Ramp, R.L. Jeffcoat, Int. J. Oral Maxillofac. Implants 16 (5) (2001) 637–645.
[17] N.C. Geurs, R.L. Jeffcoat, E.A. McGlumphy, M.S. Reddy, M.K. Jeffcoat, Int. J. Oral Maxillofac. Implants 17 (2002) 811–815.
[18] C. Aparicio, N.P. Lang, B. Rangert, Clin. Oral Implants Res. 17 (Suppl. 2) (2006) 2–7.
[19] P.-C. Chang, N.P. Lang, W.V. Giannobile, Clin. Oral Implants Res. 21 (2010) 1–12.
[20] A. Rocci, M. Martigononi, P.M. Burgos, J. Gottlow, L. Sennerby, Clin. Implant. Dent. Relat. Res. 5 (Suppl. 1) (2003) 88–98.
[21] I. Abrahamsson, T. Berglundh, J. Lindhe, J. Clin. Periodontol. 24 (1997) 568–572.
[22] O.K. Ahmed, J.R. Kelly, Int. J. Oral Maxillofac. Implants 28 (2013) 89–95.
[23] L.R. VanSchoiack, J.C. Wu, C.G. Sheets, J.C. Earthman, Mater. Sci. Eng. C 26 (2006) 1307–1311.
[24] J. Nocedal, S.J. Wright, Numerical Optimization, 2nd ed. Springer, 2006.